

Interactive comment on “A study of polarimetric noise induced by satellite motion: Application to the 3MI and similar sensors” by Souichiro Hioki et al.

Souichiro Hioki et al.

souichiro.hioki@univ-lille.fr

Received and published: 23 December 2020

We are very grateful for the reviewer’s careful and constructive comments. The comments contain insightful questions and the new perspectives that authors did not initially realize. This can be possible only through the reviewer’s profound experience and knowledge, as well as attentive reading of the manuscript. Thank you very much for the time spent in providing us useful comments. The followings are the response from the authors to those comments.

Major comment (1)-1

- The uncertainties should not be labeled as “noise”.

We agree with the reviewer to be precise in the terminology of the uncertainty. With suggestions from other reviewers, we replace the term “noise” with “error” and other appropriate terminology in the revised manuscript.

Major comment (1)-2

- It is debatable to what extent a statistical framework can accurately describe the uncertainties.

The reviewer points out that there is no random process in the mechanism of uncertainties, and therefore the statistical approach may not be the best description of the error. The authors share the same view as the reviewer, and for this reason we did not attempt to perform a parametric analysis of the distribution. The distributions (histograms and correlations) are presented to better describe the nature of the error, rather than to fit the distribution with a known simple distribution.

Major comment (1)-3

- Any distributions for low DOLP will be skewed.

For sure this is true, and the authors would like to add that any distributions for high DOLP will also be skewed.

Major comment (1)-4

- To a large extent, these systematic effects can be predicted and therefore partially mitigated, as the spatial structure that induces them is always measured.

There are two possible measurements of the spatial structure in the case of the 3MI. First is the measurement from the 3MI itself, and the other is the one from the METimage instrument that is also on the same satellite platform. The 3MI has 4 km resolution, whereas METimage has higher resolution of 500 m. The first approach, which uses only the 3MI data, is the main interest of this study. As shown in the response to the Ma-

[Printer-friendly version](#)[Discussion paper](#)

for comment (2) below, our understanding is that the effect of satellite motion is already mitigated to the first order by the linear interpolation, and our discussion is primarily on the residual error. Non-linear interpolation might indeed improve the mitigation, but it is at the expense of the spread in the modulation transfer function (i.e. blurred image). For this part, the authors admit that a dedicated study would be necessary based on the results that we obtained in this study. The second approach is important for the mitigation of the error, and we clarified the possible use of the METimage data in the discussion section of the revised manuscript.

Major comment (2)

- It remains unclear why the Laplacian is used as a proxy for the systematics instead of a regular gradient.

The authors are grateful for the reviewer's careful comment, and we are happy to take this opportunity to present what we know about the distinction between the linear term and the non-linear terms in the systematics. As the reviewer pointed out, the spurious polarization is described as the amount of uncorrected shift times the gradient + higher order terms. In other words, the values of shifted X_{m60} and X_{p60} can be written as follows:

$$X_{m60}(-s) = X_{m60}(0) - \frac{dX_{m60}}{dx}s + O(s^2) \quad (1)$$

$$X_{p60}(s) = X_{p60}(0) + \frac{dX_{p60}}{dx}s + O(s^2) \quad (2)$$

where s is the amount of shift in pixels ($0 \leq s < 1$). Without "unshifting", the L_p is computed from $X_{m60}(-s)$, $X_0(0)$ and $X_{p60}(s)$ in place of $X_{m60}(0)$, $X_0(0)$, and $X_{p60}(0)$, and therefore contains an error. The mitigation could be performed by first computing the gradient from the two measurements near 0. Note that for X_{m60} , the measurements are performed at $x = \dots, -1-s, -s, 1-s, \dots$, and for X_{p60} , at $x = \dots, -1+s, s, 1+s, \dots$.

$$\frac{dX_{m60}}{dx} = X_{m60}(1-s) - X_{m60}(-s) + \epsilon_m \quad (3)$$

$$\frac{dX_{p60}}{dx} = X_{p60}(s) - X_{p60}(s-1) + \epsilon_p \quad (4)$$

where ϵ_m and ϵ_p are errors due to the discretization. Then, Eqs. (3) and (4) are substituted into Eqs. (1) and (2):

$$X_{m60}(-s) = X_{m60}(0) - sX_{m60}(1-s) + sX_{m60}(-s) + O(s^2) + s\epsilon_m \quad (5)$$

$$X_{p60}(s) = X_{p60}(0) + sX_{p60}(s) - sX_{p60}(s-1) + O(s^2) + s\epsilon_p \quad (6)$$

The best estimates of the corrected $X_{m60}(0)$ and $X_{p60}(0)$ could be therefore defined as follows:

$$\hat{X}_{m60}(0) = (1-s)X_{m60}(-s) + sX_{m60}(1-s) \quad (7)$$

$$\hat{X}_{p60}(0) = (1-s)X_{m60}(s) + sX_{m60}(s-1) \quad (8)$$

Equations (7) and (8) are exactly the linear interpolations that we perform to obtain the unshifted X_{m60} and X_{p60} in this study. The leading error terms in Eqs. (5) and (6) are $O(s^2)$ and we therefore consider that Laplacian is the most appropriate measure of the residual error. We include a brief conclusion from this calculation in the revised manuscript, as interested readers could also refer to this Authors' Response online for full details. Of course, at your recommendation, we are ready to include this discussion as an appendix.

Major comment (3)

- Remaining pixel-to-pixel gain variations can also lead to spurious polarization signals. What do you assume for the flat-fielding calibration accuracy? And, why not take this into account in the simulation as well?

We agree with the reviewer that the remaining pixel-to-pixel gain variation can contribute to the error. In this study, however, it is not taken into consideration. The flat-fielding calibration target for the 3MI is 2% between any two pixels in a field of

Interactive
comment

Printer-friendly version

Discussion paper



view, and 0.1% for any 10×10 pixels area (Fougnie et al. 2018). As the shift is 0.45 pixels, which is way less than 10 pixels, the 0.1% is the relevant accuracy requirement. In addition, the contribution factor of the same detector element is 55% ($1 - (1.8\text{km})/(4\text{km}) = 0.55$) in the linear interpolation that unshift the X_{p60} and X_{m60} images. According to our simple estimation without spatial correlation, the 0.1% calibration error results in $p = 8.8 \times 10^{-5}$ (median) for an originally unpolarized scene with $L = 0.2$. This is significantly smaller than the error we obtained, and the actual characteristics of the residual gain between adjacent pixel is not available. We therefore didn't include the flat-field calibration error into this study.

Other comments

- It would be highly useful to list the polarimetric requirements for 3MI to put these results into context.

We appreciate this suggestion very much, along with similar suggestion by other two reviewers. It is indeed important to put the results into the context of the system requirements. To put our results into wider perspectives, we're providing here a comparison to both the previous POLDER requirements and the targeted 3MI ones. The target polarimetric accuracy of the 3MI sensor is 5×10^{-4} in terms of polarized reflectance over homogeneous clear-sky over ocean (Fougnie et al. 2018). Figure 1 shows the fraction of pixels that satisfy this condition as a function of the along-track Laplacian (black points and lines). The blue points and lines indicate the fraction of pixels that satisfy the POLDER specification, which is 1×10^{-3} in terms of polarized normalized radiance. Given that 68.2% of data falls within the $\pm 1\sigma$ when the error distribution follows the normal distribution, we could interpret that the specification is well satisfied in a particular bin when the fraction exceeds 68.2%. Over very homogeneous scenes with low along-track Laplacian, indeed we find that the requirements are satisfied, but obviously not anymore as the along-track Laplacian (i.e. inhomogeneity of the scene) increases. This result is consistent with the study by Fougnie et al. (2007), which shows that the POLDER data over homogeneous scene satisfy the requirement. In the

[Printer-friendly version](#)[Discussion paper](#)

revised manuscript, we add one paragraph that discuss this point.

- Same for the atmospheric parameters that are derived from these measurements.

It is also our interest how the polarimetric error from this study impact the derived atmospheric parameters. However, the extraction of the parameters depends significantly on the algorithm and assumption in the retrieval algorithms. In this study, we therefore prefer to stay focused on the error for the Level 1B products.

- It would be good to discuss the basics of these vicarious calibration methods.

We appreciate this comment. Some vicarious calibration methods are intended for the absolute calibration whereas others are more suited to transfer the calibration coefficients between wavelengths. We add in the revised manuscript a paragraph containing the characteristics of these methods.

- There is a mistake in Eq.5: The last factor should be X_{m60} .

Thank you very much for catching this error. We correct the equation in the revised manuscript.

- Why not consider the angle of linear polarization? And why not stick to the Stokes parameters (Q,U) or (Q/I,U/I) to keep things mathematically well-behaved.

The angle of linear polarization (AOLP) and Stokes parameters are also of an interest for certain readers. The authors agree with the reviewer that the analysis based on the Stokes parameters (Q and U) would be beneficial, particularly for the mitigation of non-linear term contributions, as Q and U are linearly related to the measured intensity. The reason why we selected the L_p and the DOLP for presentation is that they are two most frequently-used parameters in the downstream applications including the retrieval of physical quantities. In addition, the AOLP error statistics is likely more sensitive to the viewing geometry difference between the SGLI and 3MI. As the SGLI covers only a part of viewing geometry of the 3MI, we prefer to present the results for DOLP and L_p .

[Printer-friendly version](#)[Discussion paper](#)

- I don't understand the sentence on lines 69-70, "Rather, the noise tends to suppress the polarization for strongly polarized target and tends to enhance the polarization for weakly polarized target"... Maybe you should distinguish additive and multiplicative spurious polarization effects?

In the revised manuscript, we edited the sentence to make the point clearer. The sentence was to mean that noise for a scene with $DOLP \approx 0$ tends to increase the DOLP whereas a noise for a scene with $DOLP \approx 1$ tends to reduce the DOLP because the DOLP is bounded by 0 and 1.

- Please discuss in detail the commonalities and differences as hinted at in Section 2.1 between the polarimetric implementations of SGLI and 3MI. A cartoon figure may come in handy.

We appreciate the suggestion from the reviewer. We add a paragraph clarifying the commonalities and differences between the SGLI and 3MI in the revised manuscript. A cartoon figure as shown in Fig. 2 is added to highlight that the commonality is the measurement principle (three intensity measurements with linear polarizer at different angles) and the difference is the acquisition arrangements.

- Please explain the particular values in Tables 1 and 2.

The values in Table 1 is computed from the following equation:

$$w_0(i) = \frac{1}{16} \int_{i-1}^i \Pi_{4,8}(x-s) dx \quad (9)$$

where i is the index of line, $\Pi_{a,b}(x)$ is a boxcar function that is 1 in the interval (a, b) and 0 otherwise, and s is the amount of shift in SGLI pixel size (i.e. +1.8 or -1.8 in our case). This is an integral of a boxcar function in the field-of-view with a boxcar modulation transfer function. The values in Table 2 is due to the consequence of the linear interpolation near the center of image, and can be computed as follows:

$$w(i) = \left(1 - \frac{s}{4}\right)w_0(i) + \frac{s}{4}w_0(i + 4\text{sgn}(s)) \quad (10)$$

where $\text{sgn}(s)$ is sign of the shift.

- I100 Please provide some more details on what you interpolate, and how.

The reviewer points out that it is uncertain what is interpolated in the unshifting. At this stage of data processing, we have the X_{m60} and X_{p60} by aggregating 4×4 SGLI pixels, but these images are shifted by ± 1.8 SGLI pixel into the along-track direction to mimic the 3MI shift caused by sequential acquisition. For this reason, linear interpolation is necessary to obtain the X_{m60} and X_{p60} at the pixel centers of X_0 . In the revised manuscript, we make this point clearer. We hope that the addition of the equation in response to the previous question also helps to understand what is performed.

- Why is there a difference in “center of mass” between the shifted grids in Table 2?

Authors admit that it was a bit confusing because the Tables 1 and 2 are not compatible in terms of the number of lines. In the revised manuscript, we correct this issue so that the shift of the center of mass does not appear to be confusing.

- Section 2.2.2 and further: I don't understand the meaning of “stratification” in this context.

This is also mentioned by other reviewers and we correct the terminology. It was meant to infer that the computed L_p and DOLP differences are binned according to the along-track Laplacian (or that divided by L), but it was not the standard terminology. We remove this expression in the revised manuscript for clarity.

- As the cloud detection algorithm is new, it would be good to provide some numbers on false positives/negatives. What are the confidence levels for cloud (non-)detections?

The purpose of our provisional cloud mask is to separate pixels into two groups, i.e. pixels that are likely cloudy and the pixels that are likely clear-sky. Indeed it is ideal if we could provide the skill of the new cloud mask, but we believe that the development and evaluation of a cloud mask is not the scope of this paper. The criteria in Table 3 and 4 are not particularly new, and we listed all criteria so that the algorithm is well

Printer-friendly version

Discussion paper



described.

- I113 introduce all the acronyms.

Thank you for the comment. These are part of the product name that characterizes the type of the SGLI L1B products. As a name convention reference, we add a reference to the SGLI Data Users Handbook. In short, the first three letters indicate the subsystem of the SGLI instrument (“POL” for polarization, “VNR” for visible and near infrared, and “IRS” for infrared scanning subsystems), the fourth letter “D” indicates the observation mode (“D” for daytime data), and the last letter indicates the resolution (“K” for 1 km resolution, “L” for aggregated 1 km resolution).

- I suppose there is a valid reason why you select a power law of $-5/3$ (Kolmogorov)

The Kolmogorov power exponent $-5/3$ is used here because the previous studies on the cloud power spectrum use this value as a reference. Even though the original intent of the early papers were to associate the wind speed power spectrum to the marine stratocumulus cloud structure, later it was found that the value could be a representative value of spectrum power law slope even for other cloud types. We evaluate the impact of this assumption on the simulation in the discussion section.

- I145: Please provide a reference for the “observed empirical distribution function”.

It might not have been clear, but this empirical distribution function is obtained from the analysis of the SGLI data as mentioned in the sentence in the same line.

- I150-158: Why not compute this in (Q,U) over which you can actually average?

Due to the flow of the paper it may not be very clear, but our averaging is performed over X_{m60} , X_0 , and X_{p60} . The averaging over (Q,U) and the averaging over (X_{m60} , X_0 , X_{p60}) produce the same results in the authors’ understanding.

- I202: I don’t understand “0.0010 (i.e. 2.2%)”

We greatly appreciate that the reviewer spotted this. The percent value is with respect

to the median DOLP, which should be clearly marked. We also found that the value is in a bin of L_{AT} with small population, and the second digit was insignificant. Therefore, the value is corrected in the revised manuscript as follows: “about 1×10^{-3} (i.e. 2% of median DOLP, 0.041)”. The same correction applies to the part of the L_p

- It would be insightful to also present intensity and polarimetric images for typical simulated cloud scenes for particular power law distributions.

Thank you very much for the suggestion. As the simulation is performed for every 3MI pixel, the image size is 20×4 , and not suitable for the visualization. It is possible to perform a simulation for a large scene only for the illustrative purposes, as shown in Figure 3. However, we are afraid that the inconsistent figure to the simulation method introduces more confusion than the understanding. The paper by Szczap et al. (2014, Geosci. Model Dev. 7. 1779-1801) is also helpful to visualize the impact of the methodology used in the simulation of cloud fields.

Again, the authors are very grateful to the reviewer for spending a significant time to go over this manuscript and carefully providing useful comments. We hope that we addressed completely the points raised by the reviewer, but if there are further questions or suggestions, we are always happy to cover those.

Interactive comment on Atmos. Meas. Tech. Discuss., doi:10.5194/amt-2020-407, 2020.

Printer-friendly version

Discussion paper



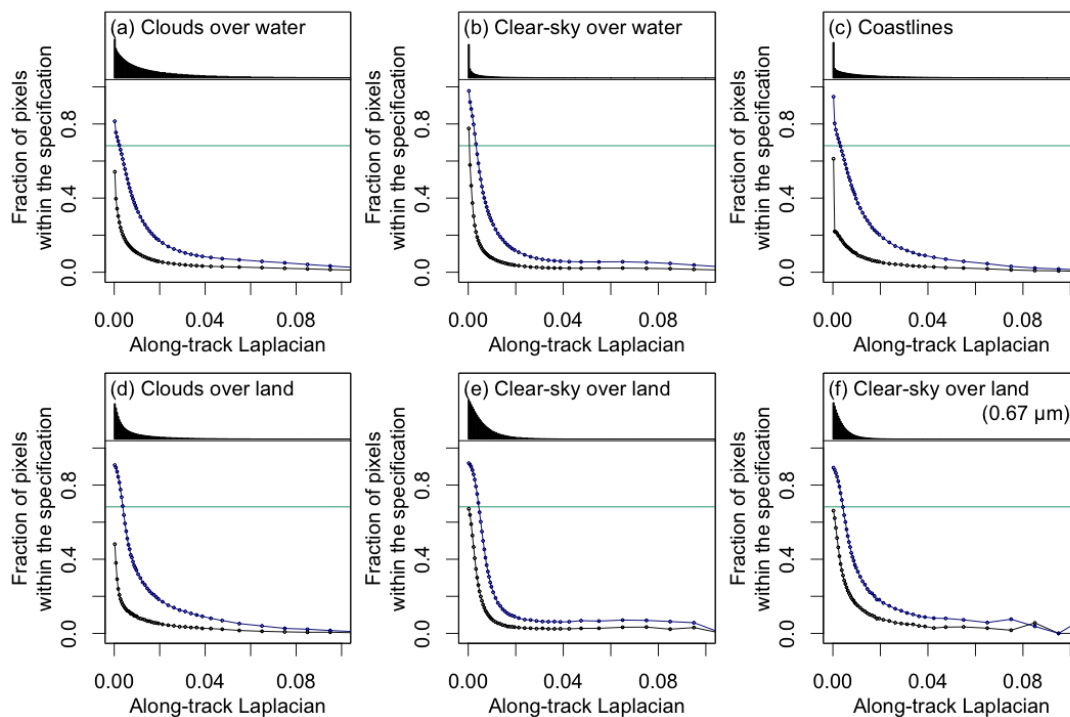


Fig. 1. Figure 1. The fraction of pixels within the POLDER specification (dark blue) and the 3MI specification (black) in each bin of along-track Laplacian. The density histograms of the along-track Laplacian

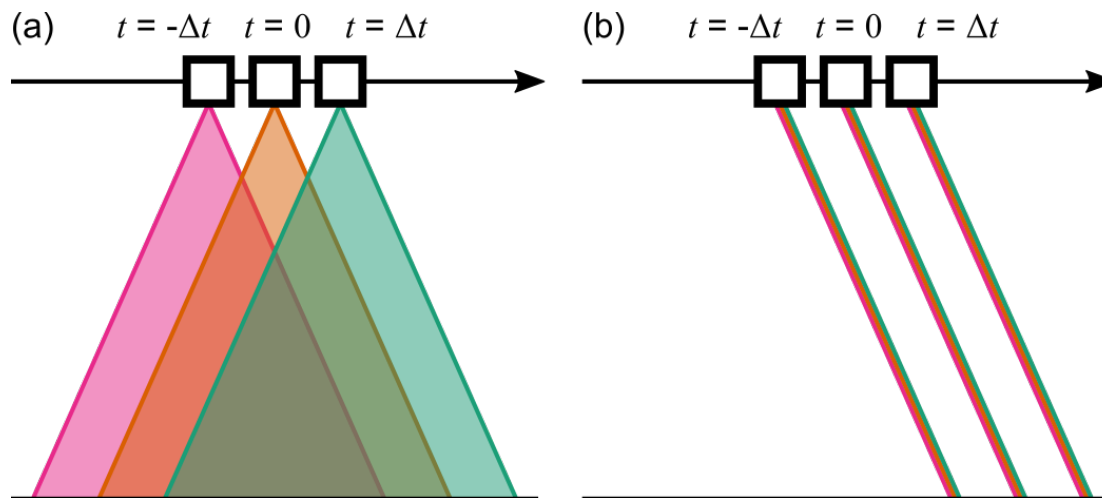


Fig. 2. Figure 2. The schematic diagram of the field-of-view by the (a) 3MI and (b) SGLI.. The black arrow shows the motion of satellite along the orbit, and the three position of the satellites along the tra

[Printer-friendly version](#)[Discussion paper](#)

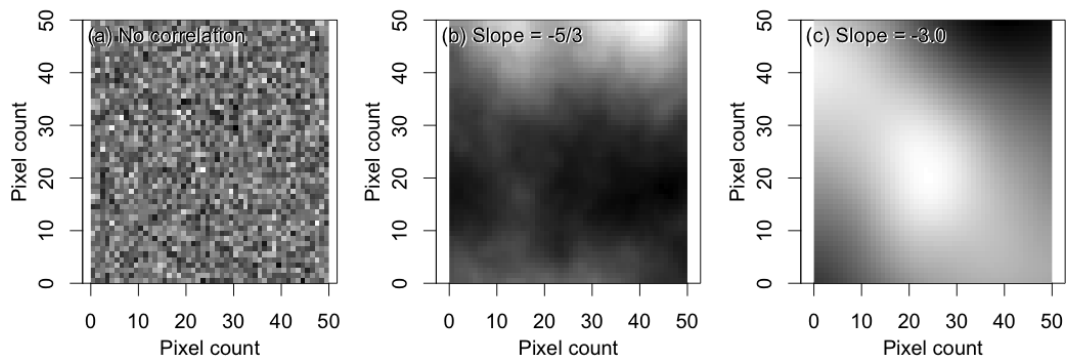


Fig. 3. Figure 3. Simulated clouds with the different power-law spectrum slope. (a) No correlation, (b) $-5/3$, and (c) -3.0 .

[Printer-friendly version](#)[Discussion paper](#)